

Running head: PHYSIOLOGICAL SYNCHRONY IN DYADIC INTERACTIONS

Methodological Advances for Detecting Physiological Synchrony During Dyadic
Interactions

Michael P. McAssey^{1,2}, Jonathan Helm², Hsieh Fushing²,
David A. Sbarra³, & Emilio Ferrer²

¹Vrije Universiteit Amsterdam, ²University of California, Davis

³University of Arizona

Abstract

A defining feature of many physiological systems is their synchrony and reciprocal influence. An important challenge, however, is how to measure such features. This paper presents two new approaches for identifying synchrony between the physiological signals of individuals in dyads. The approaches are adaptations of two recently-developed techniques, depending on the nature of the physiological time series. For respiration and thoracic impedance, signals that are measured continuously, we use Empirical Mode Decomposition to extract the low-frequency components of a non-stationary signal, which carry the signal's trend. We then compute the maximum cross-correlation between the trends of two signals within consecutive overlapping time windows of fixed width throughout each of a number of experimental tasks, and identify the proportion of large values of this measure occurring during each task. For heart rate, which is output discretely, we use a structural linear model that takes into account heteroscedastic measurement error on both series. The results of this study indicate that these methods are effective in detecting synchrony between physiological measures and can be used to examine emotional coherence in dyadic interactions.

Keywords: time series analysis, dyadic interactions, dynamical systems, psychophysiology

Methodological Advances for Detecting Physiological Synchrony During Dyadic Interactions

The synchronization of oscillatory systems – or coupled oscillations – is widely studied in the biological and physical sciences (e.g., Mirollo & Strogatz, 1990; Pikovsky et al., 2001; Weishenbush et al., 1992), with also multiple applications in the social sciences, economics, and medicine (e.g., Quian Quiroga et al., 2002). The synchrony of these oscillations can provide information about the system not available from separate univariate analyses. Consider, for example, the investigation of several electroencephalographic (EEG) signals measured simultaneously from an individual's scalp during a particular task. Each signal could be analyzed separately, and those with the most activity would indicate an area of relative activation. However, various signals can show simultaneous activation, revealing communication between different areas of the brain during the task (Engel & Singer, 2001; Fries, 2005). Furthermore, different types of such coherence – or synchrony – may be evident for different mental processes, as is the case with epileptic seizures (Quian Quiroga et al., 2002). Thus, the study of synchrony and oscillatory systems can provide a valuable means of studying psychophysiological processes, as well as possible changes in those processes as a function of different stimuli and conditions.

In the current study we propose the application of two recently developed methodologies for examining the relations between two time series. The first technique is the Empirical Mode Decomposition (EMD), an algorithm for filtering continuous time series data. The second method is the structural heteroscedastic measurement-error (SHME) model, which is adapted here for detecting linear associations between two discrete time series. We apply these techniques to physiological data from individuals in couples that participated in a laboratory-based social interaction task.

The paper is organized as follows. First, we provide a brief review of some of the common synchronization measures and their rationale in the context of emotional

processes in dyadic interactions. Second, we describe the EMD and SHME methods, with details about each of the required steps for their implementation. Third, we illustrate the application of the proposed methods with an application. The paper ends with a discussion of the potential of these models in psychophysiological research.

Synchronization Measures

Synchronization measures have become an important tool for exploring the associations between time series. Multiple methods now exist to identify and characterize synchronization, including indices of linear interdependence, such as cross-correlation, coherence, and event-related coherence, as well as more recent measures of nonlinear interdependence, such as mutual information (Kramer et al., 2004). In econometric research, for example, one of the most common methods to assess whether two series share a pattern in their long-term fluctuations is co-integration (Granger, 1981; Engle & Granger, 1987). In psychological research, perhaps the most standard method to assess synchronization consists of cross-correlations (e.g., Gottman, 1990; Mauss et al., 2005). This method can be useful to examine concurrent and lagged relations between two time series, either through the entire series or through windows of interest (e.g., Boker et al., 2002).

Synchronization of Emotion in Dyadic Interactions

Human and animal research suggests that psychophysiological linkages between two conspecifics are an inherent element of social bonding and attachment (Coan, 2008; Coan, Schaefer, & Davidson, 2006; Feldman, 2007; Gottman, Swanson, & Swanson, 2002; Guastello, Pincus, & Gunderson; Hofer, 1984, 1994; Sbarra & Hazan, 2008). The study of dyadic interactions indicates that emotional exchanges between the two members of a couple can be highly interdependent (Thompson & Bolger, 1999; Cowan & Cowan, 2000; Ferrer & Nesselroade, 2003; Ferrer & Widaman, 2008; Song & Ferrer, 2009). This research shows, for example, that the adoption of one individual's emotion state by another promotes relationship longevity (Hatfield, Cacioppo, & Rapson, 1994), that the length of

the relationship between romantic and non-romantic partners corresponds to the level of emotional coherence that the pair maintains (Anderson et al., 2003), and that the facial expression and emotional tone exhibited by romantic partners is a strong predictor of relationship dissolution (Levenson & Gottman, 1985).

Research in dyadic interactions using psychophysiological signals is scarcer. In a classic study of couples, Levenson and Gottman (1983) found that, during a conversation of disagreement, distressed couples showed significantly higher levels of synchrony between the partners' autonomic response signals than non-distressed couples. Moreover, this synchrony was predictive of marital satisfaction in the same couples. This study notwithstanding, the relative absence of research on psychophysiological synchrony in couples is conspicuous, largely because most theories of human attachment and emotion regulation suggest that the emotional experiences of one member of a couple are highly related – if not dependent upon – the experiences of his or her partner (c.f., Sbarra & Hazan, 2008). In our view, a large part of the discrepancy is methodological; theoretical developments in this area greatly outpace methodological innovations. In order to fully understand dyadic emotion regulation and psychophysiological synchrony in couples, the field needs accessible methods that can capture and adequately represent the complexity in interdependent emotional regulatory systems (Cole et al., 2004).

Synchrony between Continuous Variables: Trend Extraction using Empirical Mode Decomposition

The Empirical Mode Decomposition (EMD; Huang et al., 1998) is an algorithm developed to filter continuous data into any number of intrinsic mode functions (IMFs), each representing a particular frequency component of the original data. EMD works so that the highest-frequency components are separated out of the original time series until either no further frequency components can be detected within the residual series or a pre-set maximum number of IMFs has been extracted. These IMFs must satisfy two conditions. First, in each IMF, the total number of extrema and the total number of zero crossings must be the same or differ by one. Second, at every point in the IMF, the mean

value of the envelopes defined by the local maxima and the local minima must equal zero. These conditions are necessary for the purpose of defining the concept of instantaneous frequency in a meaningful way. The IMFs are extracted from a time series one-by-one beginning with the highest intrinsic frequency using an iterative process called *sifting*. The goal of this process is the empirical identification of intrinsic oscillatory modes in the data based on their instantaneous frequencies. The time lapse between successive extrema defines this time scale.

In the sifting process, the local maxima of the original time series are identified and connected by a cubic spline to form a curved upper envelope for the series. A lower envelope for the time series is formed in a similar way. In forming the cubic spline, adjustments at the signal boundaries must be implemented to eliminate boundary effects. The mean of the upper and lower envelopes is then computed and subtracted from the original time series to form a new series. If this new series satisfies the two IMF conditions, it is taken as the first IMF. Otherwise, the process is repeated on the new series, and so on, until the IMF conditions are satisfied. Once the first IMF is identified, it is subtracted from the original data and the residual becomes the starting point for finding the next IMF. The procedure stops when the residual signal fails to yield any suitable IMF candidates, or a pre-set maximum number of IMFs is extracted.¹

The input to the EMD is *any* continuous time series. A strong advantage of this non-parametric method is that it does not require a stationary time series in order to accomplish its task. The output from the EMD consists of a residual signal and a set of n IMFs in decreasing-frequency order. The first few IMFs cumulatively carry high-frequency components of the original time series, which are here considered to carry extraneous information riding on the actual signal of interest, which oscillates at a lower frequency. These components could be caused by associated processes, or by concurrent phenomena in the environment, or by imperfections in the recording instruments. Summing the residual and the last k IMFs together thus produces a time series that captures the information in which we are interested, while discarding extraneous information. Hence

we refer to the resulting time series as the signal of interest.

An important goal here is determining which value of k to use. The idea is to find a sufficient number of low-frequency IMFs to capture the signal that we wish to study, with some tolerance for capturing extraneous information embedded in medium-frequency IMFs. A Fast-Fourier Transform (FFT) could be used to detect the most powerful frequencies within each IMF. Then only those IMFs whose dominant frequencies are below a desired threshold are selected. However, use of the FFT is contrary to the EMD approach, since it assumes global frequencies in the signal, while EMD is devised to identify local frequencies that are not necessarily global. A better approach uses the Hilbert–Huang Transform (HHT) applied to the IMFs (Huang, 2005; Huang et al., 1998). This transform provides the amplitude and instantaneous frequency at each time point for each IMF. The energy contained in a single IMF is the sum of the squared amplitudes. Dividing this sum by the total energy of all IMFs enables us to compute the percentage of the total energy contributed by each IMF. We then select the last k IMFs such that the percentage of the total energy contributed by their combination exceeds some chosen threshold, say 90%. Adding these to the residual produces the signal of interest. See Wu and Huang (2004) and Kim et al (2008) for related applications of the HHT. Regardless of the method employed, it is informative to compare the plot of the extracted signal with that of the original signal in every case to determine whether the extracted signal appears to capture the desired trend of the original while removing sufficient extraneous information. Such a comparison may convince one to include more or fewer IMFs. For a simple example, Figure 1 shows (top panel) an obvious low-frequency sinusoidal signal with high-frequency noise. The signal of interest (bottom panel) is completely captured by adding the residual and the last three IMFs, whose combined energy is 99% of the total, while the extraneous information (the noise) is completely removed.

Once the signals of interest are extracted, the synchrony between them can then be assessed using cross-correlations. These steps are illustrated with empirical data in subsequent sections.

Synchrony between Discrete Variables: Slope Estimation using a Structural Heteroscedastic Measurement-Error Model

The SHME model is a technique to detect linear associations between discrete time series. This approach is particularly suited for capturing the relationship between two time series when the variability within each time series is not constant. The first step in the application of the SHME model consists of transforming the raw signal. For example, if the observed time series consists of electrocardiogram (EKG) data (as in the current empirical application), the raw signal is transformed into a heart rate in the form of, say, beats per minute. This can be accomplished in various ways, as is illustrated in subsequent sections.

Once the data are transformed, each of two time series are partitioned into n segments of some specified width, where n depends on the duration of the task. The choice of the segment width is a function of both detailed information and precision. Denote these segments I_1, \dots, I_n . Consider, for example, a selected time of five seconds (5000 milliseconds) for the segments. Each segment I_i will consist of m_i distinct heart rate values $x_{j,i}$, $j = 1, \dots, m_i$, for one of the series (e.g., one person's signal), each of which lasts for k_j milliseconds, and p_i distinct heart rate values $y_{j,i}$, $j = 1, \dots, p_i$ for the other series (e.g., the other person's signal), each of which lasts for l_j milliseconds. Hence $5000 = k_1 + \dots + k_{m_i} = l_1 + \dots + l_{p_i}$ for $i = 1, \dots, n$. For each segment I_i , the weighted mean heart rates are then computed as

$$u_i = \frac{1}{5000} \sum_{j=1}^{m_i} k_j x_{j,i} \quad \text{and} \quad v_i = \frac{1}{5000} \sum_{j=1}^{p_i} l_j y_{j,i}$$

for each series, respectively. Because the model requires the independence of u_1, \dots, u_n , v_1, \dots, v_n , we assume that the average heart rates in segments I_1, \dots, I_n are mutually independent for each subject.

Similarly, the weighted variance of the mean heart rate for each segment are approximated as

$$\sigma_i^2 \approx s_i^2 \sum_{j=1}^{m_i} \left(\frac{k_j}{5000} \right)^2 \quad \text{and} \quad \tau_i^2 \approx t_i^2 \sum_{j=1}^{p_i} \left(\frac{l_j}{5000} \right)^2,$$

where s_i^2 and t_i^2 are the sample variances for each time series over I_i , respectively. Since these $2n$ variances are potentially different across the two series (e.g., as in two individuals in a couple), any method for estimating the linear association between $\mathbf{u} = (u_1, \dots, u_n)$ and $\mathbf{v} = (v_1, \dots, v_n)$ must account for heteroscedastic measurement error on each variable.

The SHME model with equation error assumes that

$$u_i = \chi_i + \varepsilon_i, \quad v_i = \mu_i + \nu_i \quad \text{and} \quad \mu_i = \alpha + \beta\chi_i + \gamma_i,$$

where the independent measurement errors are $\varepsilon_i \sim \mathcal{N}(0, \sigma_i^2)$ and $\nu_i \sim \mathcal{N}(0, \tau_i^2)$, and the equation error is $\gamma_i \sim \mathcal{N}(0, \sigma^2)$. The normality of the model errors is well-justified, since the observations u_i and v_i are defined as the weighted average of independent random variables. Moreover, this model assumes that all error terms are mutually independent.

Under a structural model, both χ_i and μ_i are assumed to be random with unspecified but finite first and second moments. Note that the symmetry of this model would allow one to switch μ_i and χ_i in the latter model equation above, so that there is no implication of directionality. Techniques for estimating the slope β in this setting are available in the literature (e.g., Cheng & Riu, 2006; Kulathinal et al., 2002; Patriota et al., 2009; McAssey & Fushing, 2010). When the measurement error variance is small, as in the application here, the method-of-moments (Patriota et al., 2009) provides an efficient estimate of the slope that is simple to compute. This approach will be used to estimate β and test whether it is significantly nonzero in the empirical application.

To this end, let

$$S_{uu} = \sum_{i=1}^n \frac{(u_i - \bar{u})^2}{n-1}, \quad S_{uv} = \sum_{i=1}^n \frac{(u_i - \bar{u})(v_i - \bar{v})}{n-1}, \quad S_{vv} = \sum_{i=1}^n \frac{(v_i - \bar{v})^2}{n-1},$$

$$\sigma_n^* = \sum_{i=1}^n \frac{\sigma_i^2}{n}, \quad \tau_n^* = \sum_{i=1}^n \frac{\tau_i^2}{n}, \quad \sigma_n^{**} = \sum_{i=1}^n \frac{\sigma_i^4}{n}, \quad \text{and} \quad (\sigma\tau)_n^* = \sum_{i=1}^n \frac{\sigma_i^2 \tau_i^2}{n}.$$

Moreover, let $\sigma_\chi^2 = \text{Var}(\chi)$, $\sigma^* = \lim_{n \rightarrow \infty} \sigma_n^*$, $\sigma^{**} = \lim_{n \rightarrow \infty} \sigma_n^{**}$, $\tau^* = \lim_{n \rightarrow \infty} \tau_n^*$, and $(\sigma\tau)^* = \lim_{n \rightarrow \infty} (\sigma\tau)_n^*$. Then, having established that the distribution of $\sqrt{n}(\hat{\beta} - \beta)$ converges to $\mathcal{N}(0, \omega)$, the slope estimate $\hat{\beta}$ and its asymptotic variance ω under this model

are

$$\widehat{\beta} = \frac{S_{uv}}{(S_{uu} - \sigma_n^*)} \quad \text{and} \quad \omega = \frac{2\beta^2(\sigma^{**} - \sigma_\chi^4) + \pi}{\sigma_\chi^4},$$

where

$$\pi = \beta^2 \sigma_\chi^2 \sigma^* + \sigma^2 \sigma_\chi^2 + (\sigma\tau)^* + \sigma^2 \sigma^* + \sigma_\chi^2 \tau^* + 2\beta^2 \sigma_\chi^4.$$

Thus $\text{Var}(\widehat{\beta}) \approx \omega/n$ for n large. Substituting the parameter estimates given in Patriota et al. (2009) and simplifying, the estimated variance of $\widehat{\beta}$ is

$$\widehat{\text{Var}}(\widehat{\beta}) = \frac{2S_{uv}^2[\sigma_n^{**} - (S_{uu} - \sigma_n^*)^2]}{n(S_{uu} - \sigma_n^*)^4} + \frac{S_{uv}^2 + S_{uu}S_{vv} + (\sigma\tau)_n^* - \sigma_n^* \tau_n^*}{n(S_{uu} - \sigma_n^*)^2}.$$

The hypothesis $H_0 : \beta = 0$ will be rejected when the ratio $\widehat{\beta}/\sqrt{\widehat{\text{Var}}(\widehat{\beta})}$ deviates significantly from zero with respect to the standard normal. This procedure is illustrated with empirical data in subsequent sections.

Empirical Illustration

Measures and Procedures

The data in this study are from four couples who completed psychophysiological measurements as part of a study of dyadic interactions (see Ferrer & Widaman, 2008 for details of the study). All four couples were heterosexual with ages across all participants ranging from 26 to 32 years. The first three couples defined their relationship as “exclusively dating” and the fourth coupled as “married.” Table 1 presents information about characteristics of the individuals in the couples.

Physiological measures were collected through the MP150 physiological data collection system (BIOPAC systems) and AcqKnowledge. Stimuli were administered in a computer monitor using E-prime (Psychology Software Tools, Inc.). Three autonomic response variables were recorded from each individual within the dyad simultaneously throughout the experiment. Respiration was recorded using an elastic belt that was attached to each of the participants. The belt was placed on each subject’s chest at the point of highest extension during inhalation and exhalation. The center of the belt contained a device that recorded the level of stretch within the belt at any moment, with

greater stretch indicating inhalation and lower stretch indicating exhalation. Level of stretch within the belt was measured continuously at a rate of 1000hz.

Thoracic impedance was measured using four spot electrodes placed at the well of the neck, back of the neck, center of the chest, and center of the back. This configuration is known formally as the Qu et al., configuration (Qu, Zhang, Webster, & Thompkins, 1986). Each spot electrode came prepared with Ag/AgCl paste, and had an adhesive collar to ensure both good conductivity as well as stationarity of the electrode during the experiment. Level of impedance was measured continuously at a rate of 1000hz. An electrocardiogram was recorded using a lead II configuration, with spot electrodes on the left and right torso (bipolar leads), as well as the right collarbone (unipolar lead). All spot electrodes came prepared with Ag/AgCl paste and also had an adhesive collar. The electrocardiogram was measured continuously at a rate of 1000hz. All signals were recorded via the BIOPAC 150 and sent online to an external computer for processing and analyses. The raw signals were exported to text files and processed using the software package R (R Development Core Team, 2009) for analysis.

Participants visited a laboratory for the physiological assessment in couples. They were instructed about the experiment and completed three tasks. During the first task (Baseline task) participants were seated in comfortable armchairs and instructed to relax and refrain from making bodily movements or gestures for a period of five minutes. Sleep masks were placed over the participants' eyes and the overhead lights were turned off in order to induce an environment of relaxation. The purpose of this first task was to gain a baseline signal for each individual. During the second task (Gazing task), participants were asked to gaze into one another's eyes without talking or touching each other for three minutes. The purpose of this task was to engage the participants into an interaction that would elicit physiological arousal. During the third task (In-sync task), they were instructed to try to become in-sync with each other for three minutes. The term in-sync was described to the participants as being analogous to becoming one individual, and therefore their goal would be to match their partner's physiology. They were instructed

not to speak nor attempt physical contact during this task, but no further clarification was provided as to what constitutes being in-sync nor how to accomplish this. After the completion of the three tasks, the participants were debriefed and paid for their participation. To our knowledge, none of the couples knew any of the other couples. We never had more than one couple in the lab at any time. All aspects of this project were approved by the correspondent Institutional Review Board for the Protection of Human Subjects.

Application of EMD to Respiration and Impedance

The EMD was applied to two continuous signals, respiration and thoracic impedance. The respiration signal is a measurement of the expansion and contraction of the rib cage as the subject breathes, and thus oscillates about a fairly constant value at a varying frequency. The impedance measures the cyclical changes in cardiopulmonary output and, thus is correlated with heartbeat and respiration. Figure 2 displays the raw impedance signal for one individual (i.e., male) in Couple 3 during the first minute of the gazing task. As depicted in the figure, this time series includes considerable high-frequency oscillations riding on the underlying trend of interest.

The EMD of this impedance series produced 10 IMFs (displayed in Figure 3). Of these, only the last two IMFs were selected and added to the residual, to obtain a smoother signal. Figure 4 depicts this resulting smooth signal. Preceding IMFs could be added to obtain more detail, but at the cost of including unnecessary information. Figure 5 displays the resulting impedance signals of interest for both members of each couple during the first minute of the baseline task.

After removing the lower-frequency IMFs from each individual's time series across the three tasks, time segments of synchrony were detected between the signals of interest for the two individuals in each of the couples. For this, each pair of signals was examined using a sliding window of a fixed six-second width, which moved in two-second increments from the beginning to the end of each three- to five-minute task. This choice of the window width and the increment size is arbitrary; other choices result in equivalent

outputs but with different details. However, the six-second width was deemed reasonable to capture two or three cycles of the signals, and thereby establish a basis for detecting an occasion of synchrony between them. The two-second increments allow the detection of changes in the synchrony on a moment-to-moment level.

At each point, the cross-correlation was then computed between the signals over a range of lags, and the maximum computed value was selected as a measure of synchrony during that moment. The default lag range in R was used, which is $\pm \lfloor 10 \log_{10}(3000) \rfloor = \pm 34$. This measure is referred to as the *Instantaneous Coupling* (IC) strength. Figure 6 displays the IC series for the third couple during the baseline task with respect to their respiration (solid line) and their impedance (dashed line). Note that the two series are highly correlated, as one would expect. Moreover, there appear to be many occasions during this task when the couple’s physiological responses appears to be highly synchronized in both variables. The same phenomenon is found for the other couples.

For each of the three tasks in the experiment, the proportion $\hat{\pi}$ of IC values that exceeded a given threshold was then computed. Thresholds of 0.6 for the respiration and 0.5 for the impedance were chosen, as these values provided a reasonable baseline proportion (i.e., not too small). Finally, the proportions above the threshold for the second and third tasks were compared with that from the baseline, and a routine hypothesis test was conducted to determine whether any subsequent proportion was significantly higher than the baseline proportion. If so, it was considered as evidence of synchronization between the individuals’ physiological signals. Note that changing the threshold would alter the baseline proportion correspondingly, but it would also change the proportion for the second and third tasks by the same amount, so that the comparison of these proportions with the baseline proportion would not change. Table 2 displays the results of these analyses for respiration and impedance, for each of the four couples.

For respiration, the results indicate a significant increase in synchrony from baseline between the partners’ signals during the in-sync task, for all four couples. During the gazing task, such increase in synchrony was only evident for the first couple. With regard

to impedance, the significant increase in synchrony between the partners was perceptible during the gazing task for three of the couples, and such amplification was also true for two couples during the in-sync task.

Application of SHME to Heart Rate

In the first step, the raw EKG signal during each task was transformed into a heart rate. For this, the duration of each peak-to-peak interval of the EKG waveform (in milliseconds) was determined, and its reciprocal was used to compute the heart rate (in beats per millisecond). Then the obtained values were multiplied by 60,000 to convert them to beats per minute. Because the first recorded ventricular contraction usually does not occur in the EKG signal until after a few milliseconds, the beginning of the time series was padded with the first computed heart rate value. Similarly, because the last recorded ventricular contraction usually occurs a few milliseconds prior to the end of the EKG signal, the end of the heart rate time series was padded with the last computed value.

Figure 7 displays the resulting heart rate signals during the first 100 seconds of the baseline task for both individuals in the four couples. Note that each heart rate oscillates over a large range of values except for that of the male in the second couple, who has an almost constant heartbeat. In every case, the female's heart tends to beat faster. The objective in these analyses was to identify linear associations between the two individuals' heart rates across the experimental tasks.

For each of the tasks, the five-minute heart rate time series for both the male and female were partitioned into $n = 60$ five-second segments, following the procedure described in previous sections. The SHME model was then applied to the EKG generated data, separately for each of the four couples. The results from these analyses are presented in Table 3. These results indicate that, during the gazing task, the first couple showed a significant linear association between their heart rates. During the in-sync task, such synchrony between the partners' heart rates was evident for three couples. As expected, no synchrony was perceptible during the baseline task for any couple. We also present in Figure 8 a scatterplot of the heart rates for the first couple during each of the three tasks,

along with the fitted line bearing the estimated slope. As can be seen, the lines accurately convey the linear trajectory of each association when such an association exists.

Cross-Validation Analysis

To confirm that the discovery of synchrony in heart rate, respiration, and thoracic impedance within each of the four couples in our analyses, we applied the same methods to two mismatched couples. For this, the male from one randomly selected couple was paired with the female from another randomly selected couple as one dyad, and this process was repeated to form a second dyad. Then the analytic procedures used in the empirical analyses were implemented to detect synchrony in heart rate, respiration, and thoracic impedance of the two mismatched dyads, across the three tasks. Table 4 reports the results from these cross-validation analyses. None of the coefficients in these analyses reached significance for any measure or task (i.e., all P -values exceeding 0.1), indicating no synchrony for any of the mismatched dyads.

Discussion

Summary of Results

We presented in this paper two techniques for assessing synchrony between psychophysiological time series. For respiration and thoracic impedance, which are continuously oscillating signals, we used the EMD algorithm to filter the data and extract smooth versions of the time series. We applied a moving window to measure the maximum cross-correlation between the signals of the two individuals in the couple within the window over a lag range, and to determine when this coupling exceeded a chosen threshold. The relative frequency of high coupling values during the baseline was then compared with those during the gazing and in-sync tasks. Synchronization in respiration or impedance was inferred when the proportion of coupling occurrences increased significantly from the baseline to the experimental tasks. Our findings indicate an increase in synchrony in respiration between the partners of all four couples during the in-sync

task, relative to the baseline. Such an increase was only perceptible for one couple during the gazing task. The findings for thoracic impedance show an increase in synchrony, also relative to the baseline, during the gazing (for three couples) and the in-sync (for two couples) tasks.

For heart rate, which is measured at discrete intervals, we applied the SHME model with equation error to identify synchrony between the partners' signals. Using this approach, we estimated the slope representing the linear association between the heart rates of the two individuals in the couple during each of the three tasks. This slope was taken as an indicator of synchronization between the two partners' heart rate. Our findings indicate the presence of synchrony between the signals of three couples during the in-sync task, of one couple during the gazing task, and no synchrony at all during the baseline task. Importantly, a cross-validation analyses provided no evidence for synchrony when different members of a couple were randomly paired, thus providing evidence for the discriminative validity of these synchrony detection approaches.

Synchronization of the physiological signals was regarded as a reflection of emotional coherence between the two individuals in the couples. For example, during the in-sync task, participants might have concentrated on matching each other's breathing – as a way to mirror their partners' physiological state – thus resulting in an increase in synchrony for respiration. This effect might have carried over to the impedance (e.g., Ernst et al., 1999). Similarly, matching each other's breathing could have resulted in an increase of the coupling between the partners' heart rates. The synchrony during the gazing task can also be regarded as emotional coherence between the partners. In particular, this task was designed to elicit physiological arousal in the participants. Synchrony between the signals can then be indicative of physiological coregulation between both partners, perhaps as a way to cope with such arousal and provide ease or, more generally, showing an activation of emotional interaction between two intimate partners (e.g., Hatfield et al., 1994). Accordingly, the methods used in these analyses appear to be useful to study emotional coregulation in dyadic interactions (c.f., Sbarra &

Hazan, 2008). Finally, although we expect use individual- and dyad-level characteristics (e.g., as reported in Table 1) to predict synchrony of physiological responses (e.g., higher relationship satisfaction is related to lower physiological concordance (Levenson & Gottman, 1983)), our sample size is not large enough to detect such associations reliably.

Methodological Considerations and Future Directions

The two approaches for assessing synchrony described in this report present a number of benefits. For example, the EMD algorithm, as a tool to parse out unwanted high-frequency oscillations from continuous data, has two important advantages over other standard methods. First, it does not rely on assumptions of stationarity, assumptions required by methods such as the Fourier transform. Second, in the decomposition of the original series via EMD, there is no leakage of energy, which is common in techniques such as the wavelet transform. Moreover, in many situations, heart rate data are analyzed using methods for continuous signals. The heart rate signal, however, constitutes a step function, since it is constant on intervals between contractions. Hence, analyzing this signal as a continuous measure is not appropriate. A smoothing method could be used to transform the step function into a continuous signal, but making inferences using an imputed signal is hard to justify statistically.

A fundamental hope for the proposed statistical methods is that they can be used profitably to better understand dyadic emotion regulation and coregulation. Sbarra and Hazan (2008) recently outlined a series of analyses that would be needed in order to develop a more complete understanding of normative attachment in humans. In outlining these analyses, they wrote, “One feasible and straightforward way of testing this hypothesis would be to model the physiological functioning (e.g., indices of cardiovascular responses) of each person in a relationship as a bivariate system in which changes in one person’s physiology (in response to any task demands) are dependent on, not only their own prior physiological state, but their partner’s prior physiological state as well.” (Sbarra & Hazan, p. 157). The methods proposed here are ideally suited to answers these kinds of questions. Furthermore, many psychophysiological studies rely on collapsing data

across measurement and assessment periods. This is a reasonable approach in order to create highly reliable, epoch-specific variables, but, at the same time, it is a fundamentally limited way of studying process. When two individuals interact, it is assumed that emotional synchronization is a continuous process that is best studied in a manner that is as close to the raw data as possible. The EMD and SHME approaches allow for this type of data analysis.

One obvious extension of these analyses is the use of covariates to assess the extent to which psychophysiological synchronization is related to couple-level or individual difference variables of interest. For example, when studying intact couples, the approaches described here can be examined as a function of marital satisfaction or attachment styles, with the degree of synchronization evidenced across a study paradigm serving as an outcome variable (e.g., do more highly satisfied coupled evidence greater heart rate synchronization?) as well as a predictor of future relationship outcomes. In dyadic interaction tasks the approaches described here can be used to determine if different experimental manipulations alter the physiological synchronization or linkage between people. For instance, Butler, Wilhem, and Gross (2006) examined respiratory sinus arrhythmia as an indicator of emotion regulation during a social interaction task. In studies of this kind, the EMD and SHME approaches can be used to determine the extent to which physiological synchronization might differ across the different instructed emotion regulation tasks. These applications, of course, would require the inclusion of more couples in the sample.

Finally, this paper focused on dyadic interactions and examined the synchronization between two individuals with regard to a given physiological signal (i.e., respiration, impedance, or heart rate). Thus, this study investigated associations between two time series. An important extension of this work would involve the use of multivariate time series. For example, a pertinent question here is how to identify synchronization among multiple physiological signals, and then across the two members of a dyad. In particular, emotion researchers would be interested in examining under which conditions, and to

what extent, such multivariate coherence is most likely to emerge (e.g., Fushing et al., 2011; McAssey et al., 2010). These possible extensions notwithstanding, we hope that the methods proposed in this paper illustrate some new possibilities for studying physiological synchrony during dyadic interactions.

References

- Anderson, C., Keltner, D., & John, O.P. (2003). Emotional convergence over people over time. *Journal of Personality and Social Psychology, 84*, 1054–1068.
- Boker, S.M., Rotondo, J.L., M., & King, K. (2002). Windowed cross-correlation and peak picking for the analysis of variability in the association between behavioral time series. *Psychological Methods, 7*, 338–355.
- Cheng, C.-L., & Riu, J. (2006). On estimating linear relationships when both variables are subject to heteroscedastic measurement errors. *Technometrics, 48*, 511–519.
- Coan, J. A. (2008). Toward a neuroscience of attachment. In J. Cassidy & P. R. Shaver (Eds.), *Handbook of attachment: Theory, research, and clinical applications* (2nd ed.) (pp. 241–265). New York: Guildford Publications.
- Coan, J. A., Schaefer, H. S., & Davidson, R. J. (2006). Lending a hand: Social regulation of the neural response to threat. *Psychological Science, 17*, 1032–1039.
- Cole, P. M., Martin, S. E., & Dennis, T. A. (2004). Emotion regulation as a scientific construct: Methodological challenges and directions for child development research. *Child Development, 75*, 317–333.
- Cowan, C. P., & Cowan, P. A. (2000). *When partners become parents: The big life change for couples*. Mahwah, NJ: Lawrence Erlbaum Associates.
- Engel, A. K., & Singer, W. (2001). Temporal binding and the neural correlates of sensory awareness. *Trends in cognitive Sciences, 5*, 16–25.
- Engle, R.F., & Granger, C. W. J. (1987). Co-integration and error correction: Representation, estimation, and testing. *Econometrica, 55*, 251–276.
- Ernst, J.M., Litvack, D.A., Lozano, D.L., Cacioppo, J.T., & Berntson, G.C. (1999). Impedance pneumography: Noise as signal in impedance cardiography. *Psychophysiology, 36*, 333–338.

- Feldman, R. (2007). Parent-infant synchrony: Biological foundations and developmental outcomes. *Current Directions in Psychological Science*, *16*, 340–345.
- Ferrer, E., & Nesselroade, J.R. (2003). Modeling affective processes in dyadic relations via dynamic factor analysis. *Emotion*, *3*, 344–360.
- Ferrer, E., & Widaman, K. F. (2008). Dynamic factor analysis of dyadic affective processes with inter-group differences. In N.A. Card, J.P. Selig., & T.D. Little (Eds.), *Modeling dyadic and interdependent data in the developmental and behavioral sciences* (pp. 107–137). Hillsdale, NJ: Psychology Press.
- Fries, P. (2005). A mechanism for cognitive dynamics: Neuronal communication through neuronal coherence. *Trends in Cognitive Sciences*, *9*, 474–480.
- Fushing, H., Ferrer, E., Chen, S., Mauss, I.B., Oliver, J., & Gross, J.L. (2011). A network approach for evaluating coherence in multivariate systems: An application to psycho-physiological emotion data. *Psychometrika*, *76*, 124–152.
- Granger, C. W. J. (1981). Some properties of time series data and their use in econometric model specification. *Journal of Econometrics*, *16*, 1, 121–130.
- Gottman, J. M. (1990). Time-series analysis applied to physiological data. In J.T. Cacioppo & L.G. Tassinary (Eds.), *Principles of psychophysiology: Physical, social, and inferential elements* (pp. 754–774). New York, Cambridge University Press.
- Gottman, J., Swanson, C., & Swanson, K. (2002). A general systems theory of marriage: Nonlinear difference equation modeling of marital interaction. *Personality and Social Psychology Review*, *6*, 326–340.
- Guastello, S. J., Pincus, D., & Gunderson, P. R. (2006) Electrodermal arousal between participants in a conversation: Nonlinear dynamics and linkage effects. *Nonlinear Dynamics, Psychology, and Life Sciences*, *10*, 365–399.

- Hatfield, E., Cacioppo, J.T., & Rapson, R.L. (1994). *Emotional contagion: Cambridge studies in emotion and social interaction*. Cambridge, UK: Cambridge University Press.
- Hofer, M. A. (1984). Relationships as regulators: A psychobiological perspective on bereavement. *Psychosomatic Medicine*, *46*, 183–197.
- Hofer, M. A. (1994). Hidden regulators in attachment, separation, and loss. In N. A. Fox (Ed.), *The development of emotion regulation: Biological and behavioral considerations. Monographs of the society for research in child development* (Vol. 59(2-3), pp. 250–283).
- Huang, N.E., Shen, Z., Long, S.R., Wu, M.C., Shih, H.H., Zheng, Q., Yen, N.-C., Tung, C.C., & Liu, H.H. (1998) The Empirical Mode Decomposition and Hilbert Spectrum for nonlinear and nonstationary time series analysis. *Proceedings of the Royal Society London A.*, *454*, 903–995.
- Huang, N.E.(2005). Introduction to the Hilbert–Huang Transform and Its Related Mathematical Problems. In Huang, N.E. & Shen, S.S.P. (Eds.) *Hilbert–Huang Transform and Its Applications*, 1–25.
- Kim, D., & Oh, H.-S. (2009). EMD: A package for Empirical Mode Decomposition and Hilbert Spectrum. *The R Journal*, *1/1*, 40–46.
- Kim, D., Paek, S.H. & Oh, H.-S. (2008). A Hilbert–Huang Transform Approach for Predicting Cyber-attacks. *Journal of the Korean Statistical Society*, *37(3)*, 277–283.
- Kramer, M.A., Edwards, E., Soltani, M., Berger, M.S., Knight, R.T., & Szeri, A.J. (2004). Synchronization measures of bursting data: Application to the electrocorticogram of an auditory event-related experiment. *Physical Review E*, *70*, 011914–03.
- Kulathinal, S.B., Kuulasmaa, K., & Gasbarra, D. (2002). Estimation of an

errors-in-variables regression model when the variances of the measurement errors vary between the observations. *Statistics in Medicine*, *21*, 1089–1101.

Levenson, R.W., & Gottman, J.M. (1983). Marital interaction: Physiological linkage and affective exchange. *Journal of Personality and Social Psychology*, *45*, 587–597.

Levenson, R.W., & Gottman, J.M. (1985). Physiological and affective predictors of change in relationship satisfaction. *Journal of Personality and Social Psychology*, *49*, 85–94.

Mauss, I. B., Levenson, R. W., McCarter, L., Wilhelm, F. H., & Gross, J. J. (2005). The tie that binds? Coherence among emotional experience, behavior, and autonomic physiology. *Emotion*, *5*, 175–190.

McAssey, M., & Fushing, H. (2010). Slope estimation in structural line-segment heteroscedastic measurement error models. *Statistics in Medicine*, *29*, 2631–2642.

McAssey, M., Fushing, H., & Ferrer, E. (2010). Optimal and robust design for efficient system-wide synchronization in networks of randomly-wired neuron-nodes. *Statistics and Its Interface*, *3*, 159–168.

Mirollo, R.E., & Strogatz, S. H., (1990). Synchronization of pulse-coupled biological oscillators. *SIAM Journal on Applied Mathematics*, *50*, 1645–1662.

Patriota, A.G., Bolfarine, H., & de Castro, M. (2009). A heteroscedastic structural errors-in-variables model with equation error. *Statistical Methodology*, *6*, 408–423.

Pikovsky, A., Rosenblum, M., & Kurths, J. (2001). *Synchronization: A universal concept in nonlinear sciences*. Cambridge, UK: Cambridge University Press.

Quiñan Quiroga, R., Kraskov, A., Kreuz, T., & Grassberger, P. (2002). Performance of different synchronization measures in real data: A case study on electroencephalographic signals. *Physical Review E*, *65*, 041903-14.

- R Development Core Team (2009). R: A language and environment for statistical computing. R Foundation for Statistical Computing, Vienna, Austria. ISBN 3-900051-07-0, URL <http://www.R-project.org>.
- Sbarra, D.A. & Hazan, C. (2008). Coregulation, dysregulation, self-regulation: An integrative analysis and empirical agenda for understanding adult attachment, separation, loss, and recovery. *Personality and Social Psychology Bulletin*, *12*, 141–167.
- Song, H., & Ferrer, E. (2009). State-space modeling of dynamic psychological processes via the Kalman smoother algorithm: Rationale, finite sample properties, and applications. *Structural Equation Modeling*, *16*, 338–363.
- Thomson, A., & Bolger, N. (1999). Emotional transmission in couples under stress. *Journal of Marriage & the Family*, *61*, 38–48.
- Weishenbush, C., Nishioka, M., Ishikawa, A., & Arakawa, Y. (1992). Observation of the coupled excitation-photon mode splitting in a semiconductor quantum microactivity. *Physical review letters*, *69*, 23, 3314.
- Wu, Z. & Huang, N.E. (2004). A study of the characteristics of white noise using the empirical mode decomposition method. *Proceedings of the Royal Society A*, *460*, 1597-1611.

Appendix

R Code for obtaining the Empirical Mode Decomposition of a time series and extracting its trend.

```

library(EMD) ## load EMD package previously installed
EMDResult <- emd(Series, boundary="wave", plot.imf=FALSE)
  ## choose "wave boundary condition; to plot IMFs, change to TRUE
Freq <- rep(0, EMDResult$nimf) ## Identify the frequency having the
  ## most power for each IMF
for(i in 1:EMDResult$nimf) {
  Pgram <- spec.pgram(EMDResult$imf[,i], taper=0, plot=FALSE)
  Freq[i] <- min(Pgram$freq[which(Pgram$spec == max(Pgram$spec))])
} ## Identify the last IMF whose strongest frequency is above a
  ## threshold of 0.002
M <- min(max(which(Freq > 0.002)), EMDResult$nimf-1)
Trend <- EMDResult$residue ## Add the latter IMFs to the residual
for(i in (M+1):EMDResult$nimf) Trend <- Trend + EMDResult$imf[,i]
  ## Trend contains the signal of interest

```

Author Note

This work was supported in part by grants from the National Science Foundation (BCS-05-27766 and BCS-08-27021) and NIH-NINDS (R01 NS057146-01). Address correspondence to Emilio Ferrer, Department of Psychology, University of California, Davis, CA 95616-8686. Email: eferrer@ucdavis.edu.

Notes

¹Kim and Oh (2009) have developed an R package called **EMD** that implements this procedure very efficiently. The R code used in these analyses is provided in the appendix.

Table 1

Individual- and Dyad-Level Characteristics of the Four Couples

Variable	Couple	Male	Female
Attachment-related avoidance (1-7 Likert scale)	1	2.33	3.67
	2	2.61	1.39
	3	3.56	2.06
	4	1.56	1.06
Attachment-related anxiety (1-7 Likert scale)	1	2.78	3.72
	2	3.22	1.94
	3	2.78	4.39
	4	2.61	2.06
Relationship satisfaction (1-7 Likert scale)	1	6.17	6.67
	2	6.00	6.83
	3	6.83	6.17
	4	6.50	6.83
Relationship status	1	Exclusively dating	
	2	Exclusively dating	
	3	Exclusively dating	
	4	Married	
Relationship length (months)	1	41	
	2	53	
	3	08	
	4	71	

Table 2

Significant Increase in Relative Frequency of Strong Instantaneous Coupling Across Tasks

Couple	Task	Respiration $\hat{\pi}$	<i>P</i> -value	Impedance $\hat{\pi}$	<i>P</i> -value
1	baseline	0.149	—	0.020	—
	gazing	0.239	0.048 *	0.102	0.008 **
	in-sync	0.886	0.000 ***	0.011	0.709
2	baseline	0.068	—	0.007	—
	gazing	0.125	0.080	0.045	0.048 *
	in-sync	0.659	0.000 ***	0.364	0.000 ***
3	baseline	0.236	—	0.122	—
	gazing	0.125	0.988	0.045	0.986
	in-sync	0.818	0.000 ***	0.375	0.000 ***
4	baseline	0.216	—	0.027	—
	gazing	0.114	0.984	0.148	0.001 ***
	in-sync	0.841	0.000 ***	0.000	0.979
0.05 < * < 0.01 < ** < 0.001 < ***					

Table 3

Slope Estimates for Association between Heart Rates Using the SHME Model Across Tasks

Couple	Task	$\hat{\beta}$	$\sqrt{\widehat{\text{Var}}(\hat{\beta})}$	<i>P</i> -value
1	baseline	0.003	0.274	0.993
	gazing	1.071	0.212	0.000 ***
	in-sync	1.344	0.626	0.032 *
2	baseline	0.358	0.703	0.610
	gazing	0.504	0.436	0.248
	in-sync	0.579	0.473	0.221
3	baseline	-0.089	0.079	0.254
	gazing	0.171	0.099	0.083
	in-sync	0.369	0.149	0.013 **
4	baseline	-0.142	0.185	0.445
	gazing	-0.227	0.961	0.813
	in-sync	0.497	0.239	0.037 *
0.05 < * < 0.01 < ** < 0.001 < ***				

Table 4

Measures of Synchrony between Heart Rates, Respiration and Thoracic Impedance for Mismatched Couples Across Tasks

Mismatched Couple	Task	$\hat{\beta}$	$\sqrt{\widehat{\text{Var}}(\hat{\beta})}$	P -value
1	baseline	-11.525	12.356	0.823
	gazing	0.250	0.206	0.117
	in-sync	-54.825	482.732	0.545
2	baseline	0.000	0.001	0.500
	gazing	0.023	0.022	0.151
	in-sync	0.000	0.021	0.500

Mismatched Couple	Task	Respiration $\hat{\pi}$	P -value	Impedance $\hat{\pi}$	P -value
1	baseline	0.095	—	0.041	—
	gazing	0.091	0.538	0.011	0.930
	in-sync	0.148	0.118	0.080	0.119
2	baseline	0.230	—	0.108	—
	gazing	0.091	0.999	0.045	0.968
	in-sync	0.216	0.598	0.114	0.448

Figure Captions

Figure 1. Original signal (top) consisting of high-frequency oscillations riding on a low-frequency signal of interest, and the low-frequency signal of interest (bottom) created by summing the last 3 IMFs and the residual.

Figure 2. Male's impedance signal during gazing task, for Couple 3.

Figure 3. IMFs produced by EMD of male's impedance signal during gazing task.

Figure 4. Male's impedance signal during gazing task, after higher-frequency IMFs are removed.

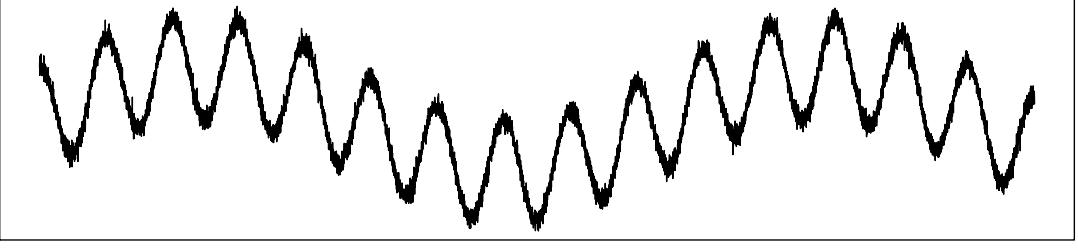
Figure 5. Impedance for the male (dark) and the female (light) during the baseline task for each couple, after higher-frequency IMFs are removed.

Figure 6. IC strength for Couple 3 during baseline task, with respect to respiration (solid line) and impedance (dashed line).

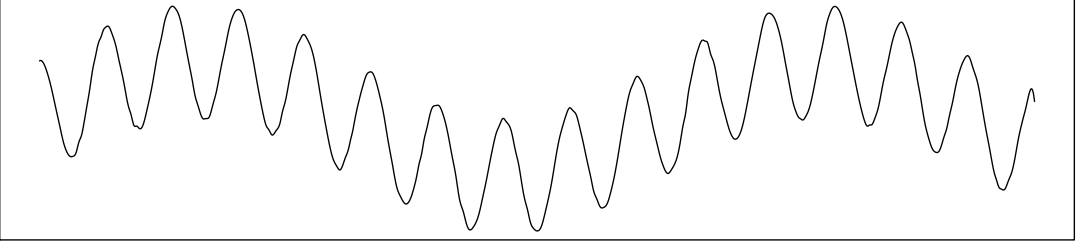
Figure 7. Heart Rate for the male (dark) and the female (light) during the baseline task for each couple.

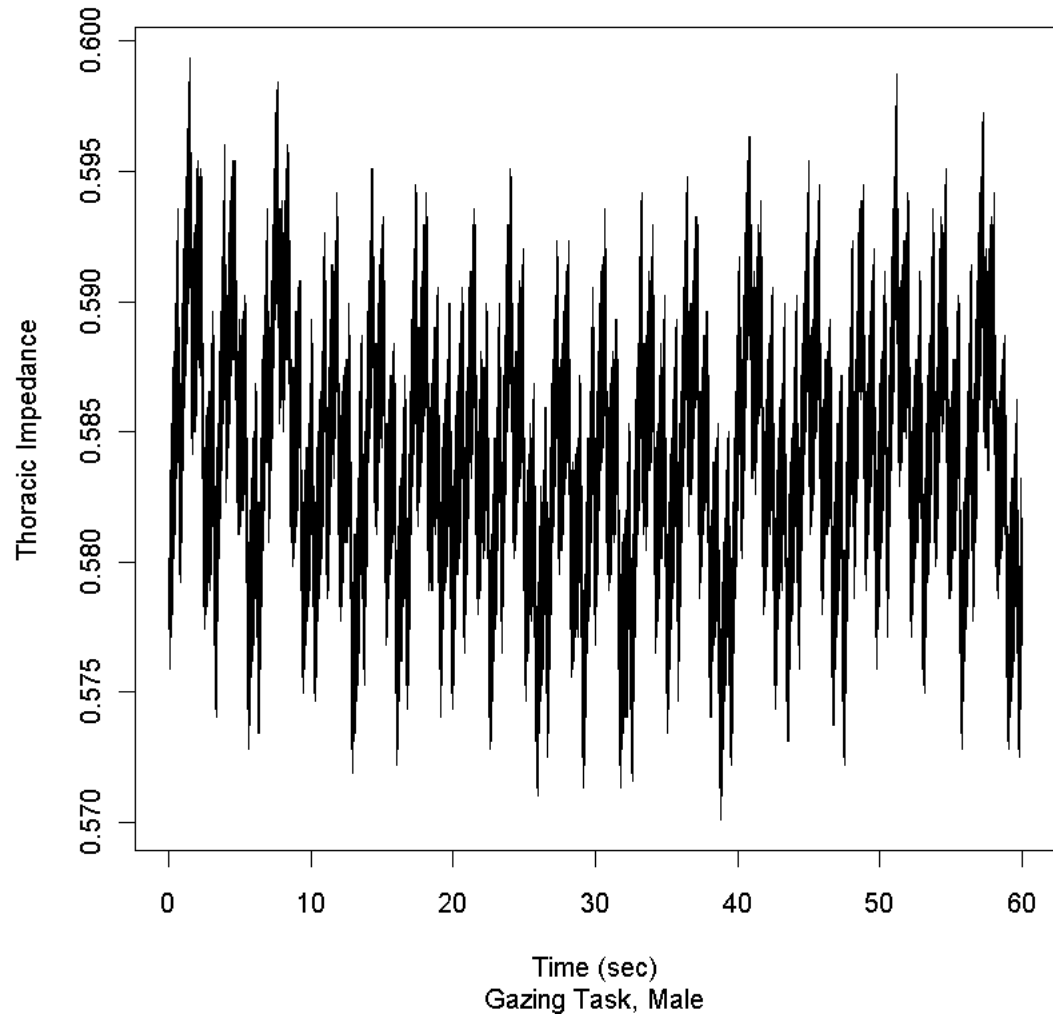
Figure 8. Scatterplots of the heart rates for the first couple during each task, with the corresponding best-fit lines.

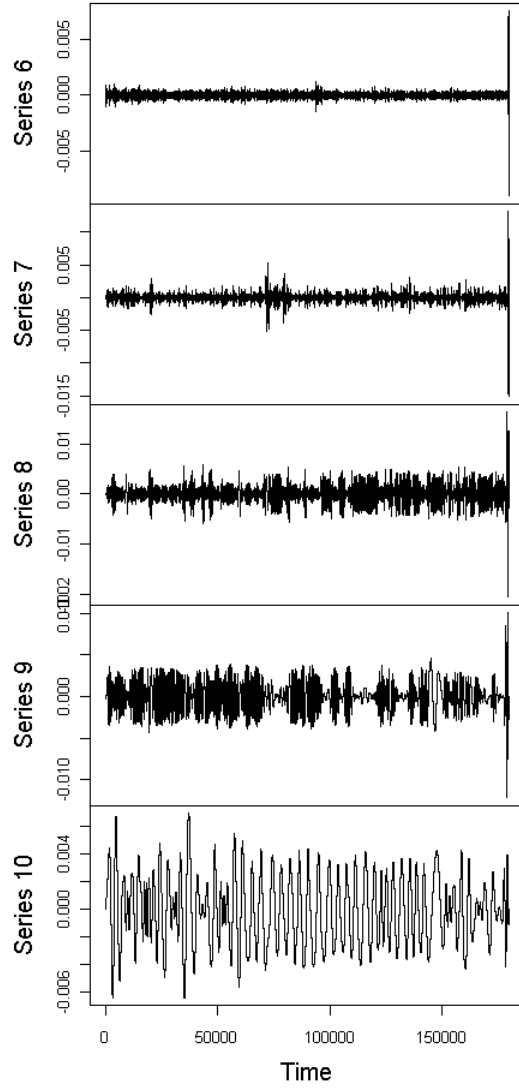
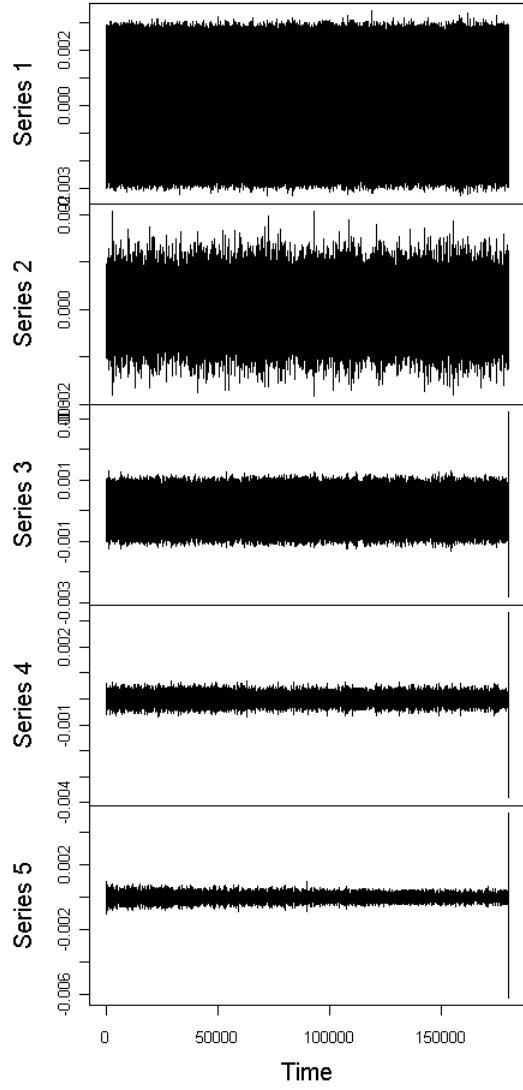
Original

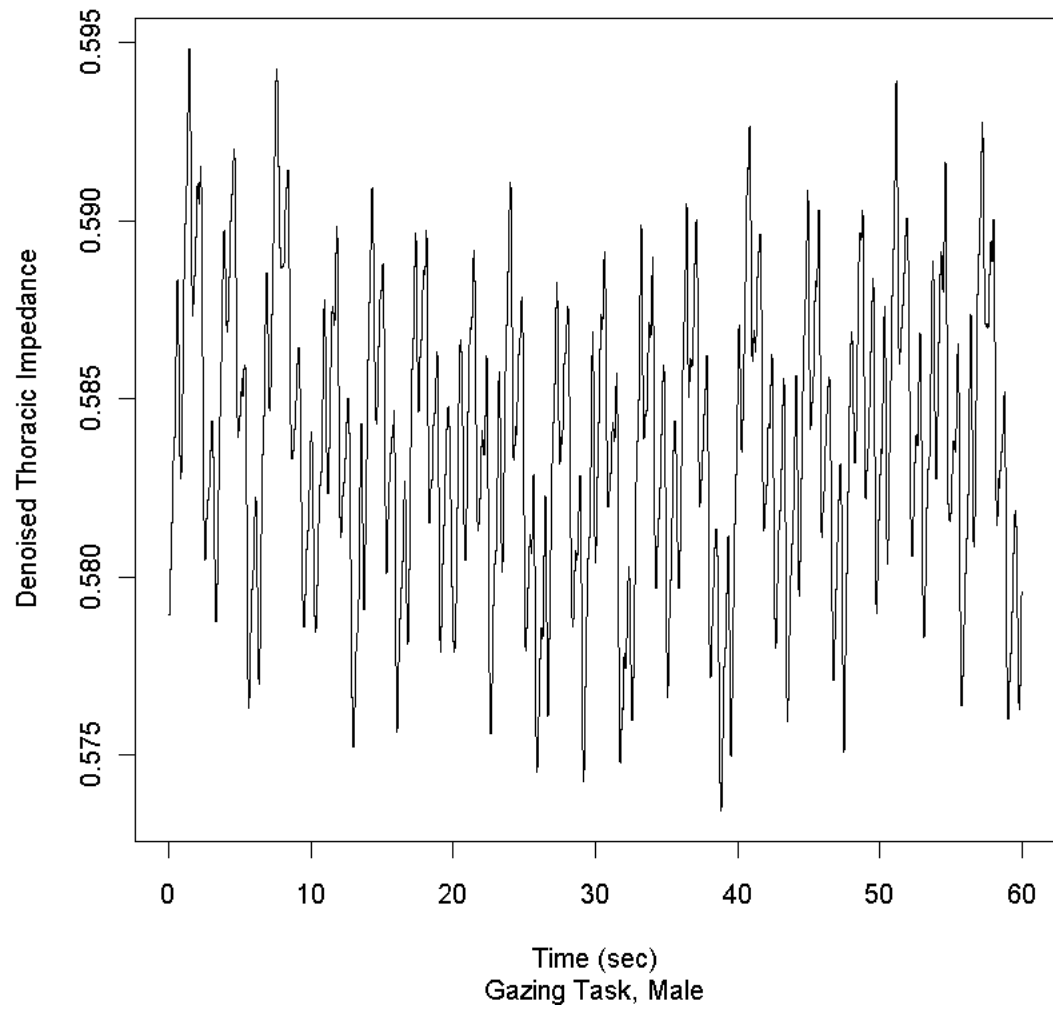


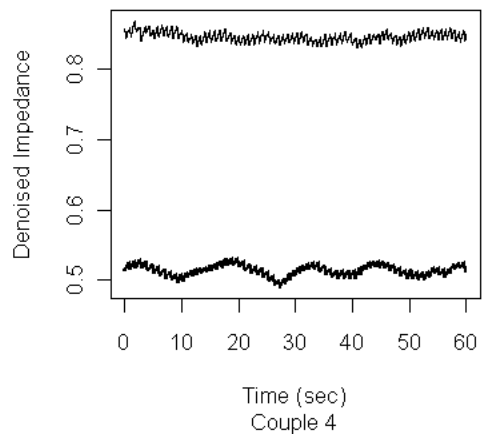
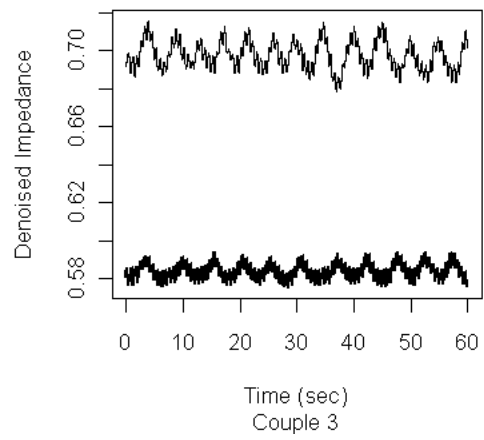
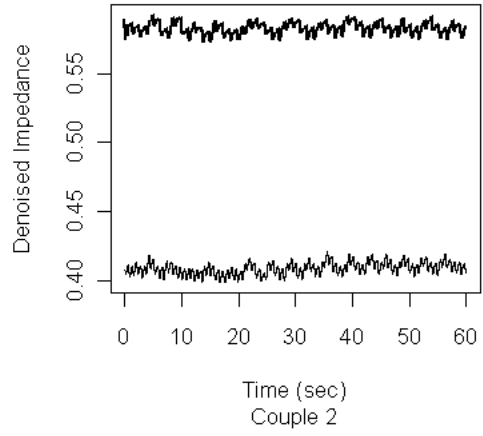
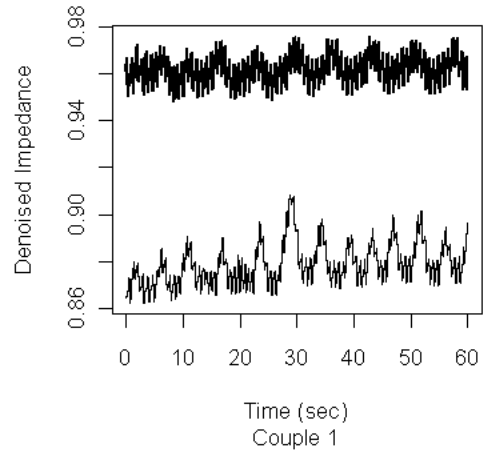
Extracted

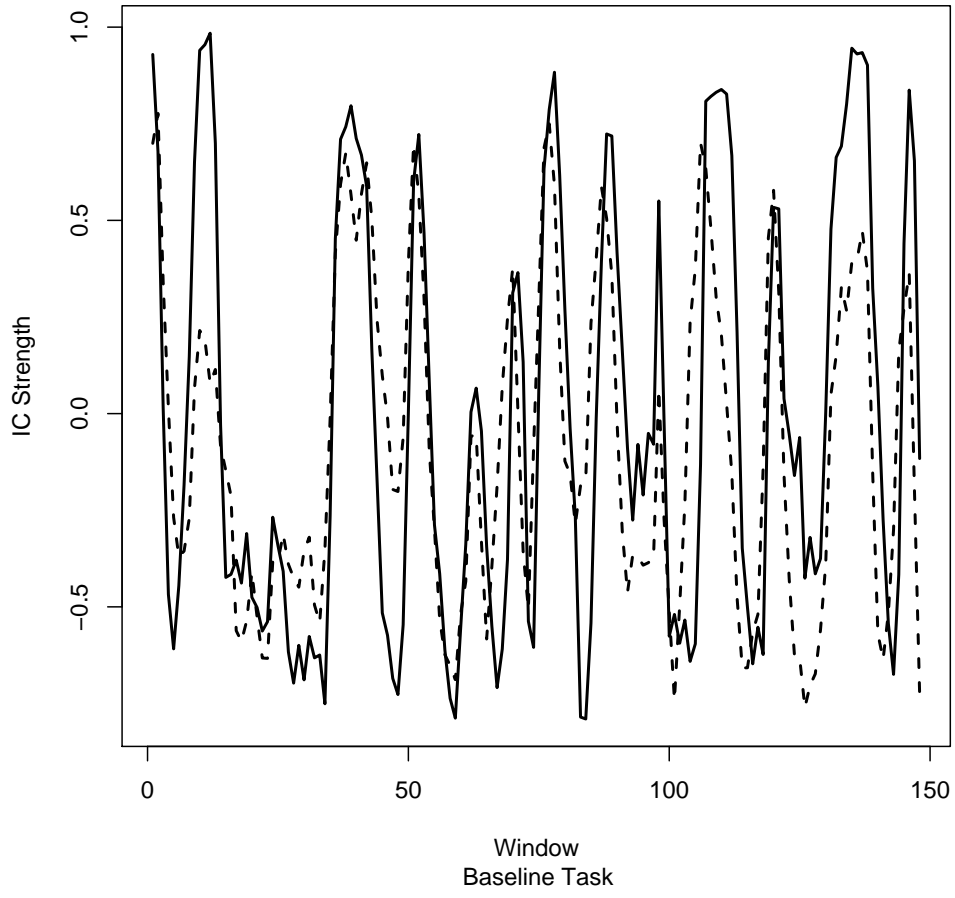


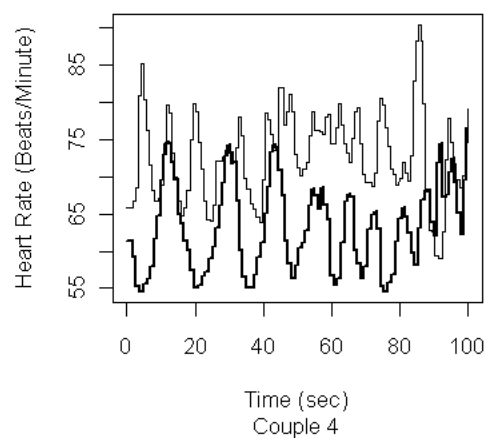
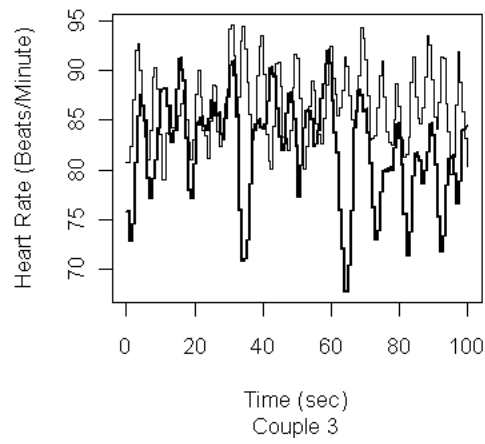
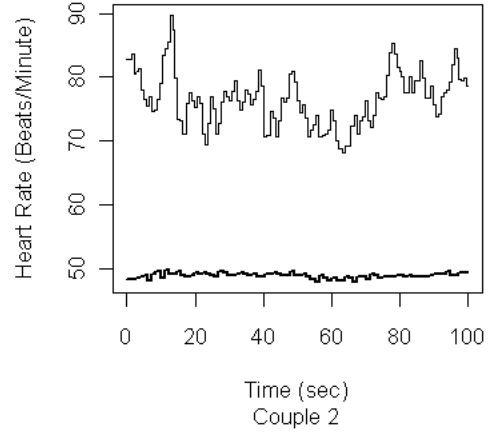
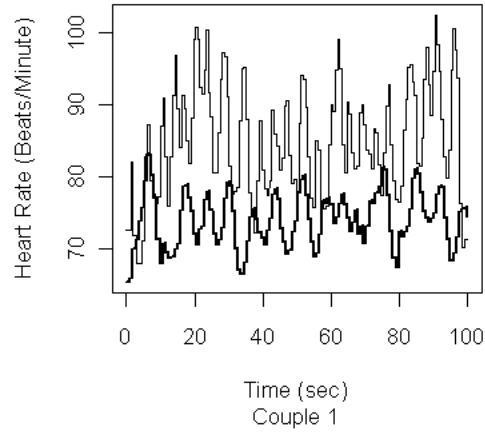




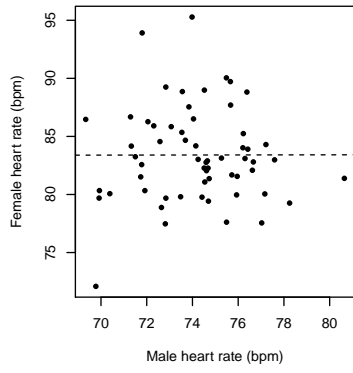




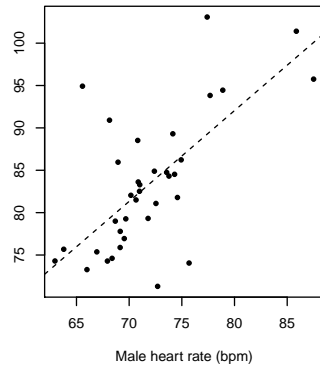




Baseline task



Gazing task



In-sync task

